



HAL
open science

Thermal signatures identify the influence of dams and ponds on stream temperature at the regional scale

Hanieh Seyedhashemi, Florentina Moatar, Jean-Philippe Vidal, Jacob Diamond, Aurélien Beaufort, André Chandesris, Laurent Valette

► To cite this version:

Hanieh Seyedhashemi, Florentina Moatar, Jean-Philippe Vidal, Jacob Diamond, Aurélien Beaufort, et al.. Thermal signatures identify the influence of dams and ponds on stream temperature at the regional scale. *Science of the Total Environment*, 2021, 766, pp.1-13. 10.1016/j.scitotenv.2020.142667. hal-03120642

HAL Id: hal-03120642

<https://hal.science/hal-03120642>

Submitted on 13 Feb 2023

HAL is a multi-disciplinary open access archive for the deposit and dissemination of scientific research documents, whether they are published or not. The documents may come from teaching and research institutions in France or abroad, or from public or private research centers.

L'archive ouverte pluridisciplinaire **HAL**, est destinée au dépôt et à la diffusion de documents scientifiques de niveau recherche, publiés ou non, émanant des établissements d'enseignement et de recherche français ou étrangers, des laboratoires publics ou privés.



Distributed under a Creative Commons Attribution - NonCommercial 4.0 International License

1 Thermal signatures identify the influence of dams and ponds on stream temperature at
2 the regional scale

3 Hanieh Seyedhashemi^{a,b*}, Florentina Moatar^a, Jean-Philippe Vidal^a, Jacob S.
4 Diamond^{a,b}, Aurélien Beaufort^{a,b}, André Chandesris^a, Laurent Valette^a

5 ^aINRAE, UR RiverLy, centre de Lyon-Villeurbanne, 5 rue de la Doua CS 20244,
6 69625 Villeurbanne, France

7 ^bEA 6293 GéoHydrosystèmes COntinentaux, Université François-Rabelais de Tours,
8 Parc de Grandmont, 37200 Tours, France

9 *Corresponding author: hanieh.seyedhashemi@inrae.fr

10 Florentina Moatar: florentina.moatar@inrae.fr

11 Jean-Philippe Vidal: jean-philippe.vidal@inrae.fr

12 Jacob S. Diamond: jacob.diamond@inrae.fr

13 Aurélien Beaufort: aurelien.beaufort@hotmail.fr

14 André Chandesris: andre.chandesris@inrae.fr

15 Laurent Valette: laurent.valette@inrae.fr

16

17 **1 Abstract**

18 Anthropogenic impoundments (e.g. large dams, small reservoirs, and ponds) are
19 expanding in number globally, influencing downstream temperature regimes in a diversity
20 of ways that depend on their structure and position along the river continuum. Because of
21 the manifold downstream thermal responses, there has been a paucity of studies
22 characterizing cumulative effect sizes at the catchment scale. Here, we introduce five
23 thermal indicators based on the stream-air temperature relationship that together can
24 identify the altered thermal signatures of dams and ponds. We used this thermal signature
25 approach to evaluate a regional dataset of 330 daily stream temperature time series from
26 stations throughout the Loire River basin, France, from 2008–2018. This basin (10^5 km²)
27 is one of the largest European catchments with contrasting natural and anthropogenic
28 characteristics. The derived thermal signatures were cross-validated with several known
29 catchment characteristics, which strongly supported separation into dam-like, pond-like
30 and natural-like signatures. We characterize the thermal regime of each thermal signature
31 and contextualize it using a set of ecologically relevant thermal metrics. Results indicate
32 that large dams decreased summer stream temperature by 2°C and delayed the annual
33 stream temperature peak by 23 days relative to the natural regimes. In contrast, the
34 cumulative effects of upstream ponds increased summer stream temperature by 2.3°C and
35 increased synchrony with air temperature regimes. These thermal signatures thus allow for
36 identifying and quantifying downstream thermal and ecological influences of different
37 types of anthropogenic infrastructures without prior information on the source of
38 modification and upstream water temperature conditions.

39 *Keywords: thermal regime, impoundment, reservoir, Loire River, thermal*
40 *sensitivity*

41 **1. Introduction**

42 *1.1 Stream temperature in a changing world*

43 River corridors store, transform, and convey mass and energy from headwaters to
44 oceans. Although rivers are typically analyzed as lotic systems, the distribution of lentic
45 water bodies (e.g., lakes, reservoirs, ponds) along the river continuum has recently come
46 to light as a critical factor in nitrogen removal (Harrison et al., 2009; Schmadel et al.,
47 2018), and storage of phosphorus (Grantz et al., 2014) and sediments (Vörösmarty et al.,
48 2003). An emerging concern is the cumulative effects of lentic systems on stream and
49 river water temperature, which is a critical parameter affecting the eutrophication of water
50 bodies (Minaudo et al., 2018; Le Moal et al., 2019) and the distribution of aquatic
51 communities (Cox & Rutherford, 2000; Poole & Berman, 2001; Ducharme, 2008).

52 Stream temperature effects from lentic water bodies depend strongly on their
53 individual characteristics and their overall spatial distributions, complicating scales of
54 inference and prediction. For example, anthropogenic features like dams, impoundments
55 and ponds appear to have contrasting effects on stream temperature (Webb, 1996; Webb
56 et al., 2008; Olden & Naiman, 2010). It is important to develop a more general
57 understanding of these effects because global change will likely exacerbate them, e.g., by
58 increasing the number of future dams or ponds and increasing the capacity of current
59 ones. Indeed, in some countries, recurrent droughts led to an increase in the number of
60 small farm dams storing water for later use in irrigation (Habets et al., 2013). The
61 preponderance of studies on the regional scale effects of anthropogenic structures use
62 physical process-based models that are highly parameterized (Van Vilet et al., 2012;
63 Niemeyer et al., 2018; Yearsley et al., 2019; Cheng et al., 2020), limiting their broad
64 applicability (Dugdale et al., 2017). Hence, there is a need for simpler, data-based tools
65 that can identify and predict such anthropogenic effects on stream temperature and

66 subsequent consequences to ecosystems, particularly at large scales relevant to
67 management.

68 *1.2 Large dams tend to reduce stream temperature and shift annual cycles*

69 The effects of large dams on river thermal regimes are well studied at the site scale
70 (Webb & Walling, 1993, 1996, 1997; Lowney, 2000; Preece & Jones, 2002; Casado et al.,
71 2013). These studies typically compare observed stream temperature regimes above and
72 below the dam, before and after dam construction, or in regulated and unregulated
73 streams, with unregulated streams being located in close proximity of regulated streams
74 with a similar climate. Results provide strong support that large dams generally reduce
75 downstream temperatures by releasing cold, hypolimnetic water in summer (Olden &
76 Naiman, 2010), and that they delay the annual cycle of both flow (Lehner et al., 2011) and
77 stream temperature regimes (Webb & Walling, 1993; Webb, 1996). Additionally, through
78 discharge regime regulation (Petts & Gurnell, 2005), large dams may also modify stream
79 temperature through the impact on thermal capacity without necessarily modifying the
80 components of heat budget (Webb & Walling, 1996; Poole & Berman, 2001). While some
81 subsequent works have used physical process-based models to upscale these effects across
82 river networks and regions (Van Vliet et al., 2012; Niemeyer et al., 2018; Cheng et al.,
83 2020; Daniels & Danner, 2020), large-scale empirical assessments remain scarce (but see
84 Steel & Lange, 2007; Maheu et al., 2016a, Hill et al., 2013). Hence, there is still a major
85 gap in our regional scale understanding of dam-induced alterations, largely because the
86 changes to any one component of river thermal regime depend on the spatiotemporal
87 scales considered (Steel & Lange, 2007).

88 *1.3 Ponds and shallow reservoirs tend to increase stream temperature*

89 Pond and shallow (<15 m in height) reservoir effects on stream temperature differ
90 from those of large dams due to their mode of downstream water release. Observations

91 suggest that the surficial water release from these structures – as opposed to hypolimnetic
92 release from large dams – tends to increase downstream stream temperature (Sinokrot et
93 al., 1995; Maxted et al., 2005; Bae et al., 2016; Maheu et al., 2016b; Chandesris et al.,
94 2019). The greatest increase in stream temperature occurs during low-flow periods
95 (Webb, 1996). Specifically, these structures increase not just the average stream
96 temperature, but also its diurnal range and the frequency and duration of high
97 temperatures (Maheu et al., 2016a, 2016b; Chandesris et al., 2019). Further, the increase
98 in downstream temperature is weakly compensated by natural processes, leading to
99 minimal downstream recovery to baseline temperatures (Boon & Shires, 1976; Fraley,
100 1979; Maxted et al., 2005; Dripps & Granger, 2013). However, thermal alterations from
101 small impoundments are far less studied than those of large dams, and their cumulative
102 effects on river thermal regimes at the regional scale are unknown.

103 *1.4 The stream-air temperature relationship as a diagnostic tool*

104 A major challenge in the regional assessment of water temperature is the lack of
105 detailed information about the heat budget (Webb & Zhang, 1997). This issue leads to
106 using air temperature as a proxy for computing the river heat budget. Simple linear
107 regression between water and air temperature is a common proxy technique to infer
108 stream thermal regimes (Stefan & Preud'homme, 1993; Pilgrim et al., 1998; Mohseni et
109 al., 1999; Erickson & Stefan, 2000; Caissie et al., 2004), but regression parameters are
110 highly spatially variable. For instance, river reaches without groundwater input typically
111 have steep regression slopes with low intercepts, but opposite relations can emerge for
112 groundwater-dominated reaches (Caissie, 2006; O'Driscoll & DeWalle, 2006; Kelleher et
113 al., 2012). The relationship between water temperature and air temperature may also be
114 altered by different types of anthropogenic disturbances leading to a weaker correlation
115 and/or a smaller regression slope (Erickson & Stefan, 2000; Webb et al., 2008; Bae et al.,

116 2016). We can therefore take advantage of these spatially variable relationships to infer
117 the controls and drivers of stream temperature.

118 *1.5 Thermal signatures as a means of identifying anthropogenic influences*

119 We suggest development of “thermal signatures” based on air-water temperature
120 relationships to identify anthropogenic influences on stream temperature regimes. The
121 choice of the name thermal signatures derives from the analogous concept of hydrological
122 signatures (Gupta et al., 2008), which use statistical analysis of flow regimes to provide
123 information on broader controls on hydrological behavior (e.g., dominant flow processes,
124 strength and spatiotemporal variability of the rainfall–runoff response (Berhanu et al.,
125 2015; McMillan et al., 2017). Similarly, thermal signatures capitalize on indicators
126 extracted from the statistical structure of local stream-air temperature relationships to
127 identify the dominant processes (e.g., anthropogenic influences) that generate observed
128 stream temperature time series. Due to the wide availability of air temperature data and
129 the rapid growth of water temperature datasets, thermal signatures can be applied at large
130 scales, facilitating regional assessments of stream temperature variability. Thermal
131 signatures further allow tracing of systematic changes introduced by anthropogenic
132 structures like dams or ponds, and identification of highly influenced reaches at large
133 scale.

134 *1.6 Purpose of the study*

135 The purpose of this study is to distinguish the characteristics of altered and natural
136 stream thermal regimes, and to determine their spatial distributions at a regional scale with
137 a simple, data-based approach. To do so, we use novel thermal signatures based on both
138 stream-air temperature linear regression and seasonality analysis. These signatures reveal
139 the influence of dams and ponds on thermal regimes without prior information on the
140 source of modification or upstream water temperature conditions. We then cross validate

141 our thermal signature approach with known properties of catchments and anthropogenic
142 structures. Finally, we contextualize the thermal signatures with a set of ecologically
143 relevant thermal metrics.

144 **2 Study area and data**

145 *2.1 Loire basin and surface waters*

146 The Loire basin is a large European catchment (10^5 km^2) with contrasting natural
147 conditions (Figure 1), providing an ideal case study to test the limitations of the thermal
148 signature approach. Mean annual precipitation (549–2130 mm), mean annual air
149 temperature (6.0–12.5°C), altitude (10–1850 m), and lithology provide spatially variable
150 controls on stream temperature regime (Figure 1, left panel.).

151 [Figure 1 about here.]

152 Surface waters (as identified by aerial photography; minimum resolution of 15 m^2)
153 cover approximately 0.8% of the Loire basin, and include 11 natural lakes and numerous
154 artificial ponds, shallow reservoirs ($6 \text{ m} < \text{height} < 15 \text{ m}$), and large dams ($\text{height} > 15 \text{ m}$).
155 Up to 70% of surface waters have surface areas less than 10 ha, and less than 0.5% of the
156 surface waters (by number) are shallow reservoirs. Hence, over 99% of surface waters are
157 artificial ponds, commonly dedicated to irrigation or recreation. Height and volume
158 estimates are unavailable for the most of these artificial ponds (see Figure 1, right panel;
159 IGN, 2006). Based on these observations, we considered surface waters that were not
160 natural lakes or dams to be “ponds”, while recognizing that some small proportion of
161 these so-called ponds may indeed be shallow reservoirs.

162 The Loire River basin houses 73 large dams (total storage capacity, $S=999 \text{ Mm}^3$),
163 which are used for hydroelectricity ($S=734 \text{ Mm}^3$), drinking water ($S=57 \text{ Mm}^3$), recreation
164 ($S=32 \text{ Mm}^3$) and navigation ($S=234 \text{ Mm}^3$) (see Figure 1, right panel). The two largest
165 dams are: 1) Naussac dam ($S=190 \text{ Mm}^3$, height =50 m), and 2) Villerest dam ($S=106$

166 Mm³, height = 59 m) (Figure 1, right panel) These large dams are located in the upstream
167 part of the basin (referred to as region A in Figure 1, right panel), with granite and basalt
168 lithology and little influence of groundwater input.

169 2.2 *Observed stream and air temperature data*

170 We obtained hourly water temperature for 2008–2018 at 392 stations with complete
171 year data, most of which were managed by the French Agency for Biodiversity
172 (<http://www.naiades.eaufrance.fr>) and the National Fishing Federation
173 (<https://www.federationpeche.fr>). Most stations (55%) had at least 5 years of data, with
174 1% having all 11 years of complete temperature data and 33% having less than 3 years.
175 The stations are evenly distributed across the Loire basin, with a median Euclidean
176 distance between any two stations of 4 km. The stations represent a wide range of river
177 discharge (mean annual specific discharge 72–1050 mm y⁻¹) and width (1.5–34 m), with
178 75% of the stations located on rivers with a Strahler order from 2 to 4. The mean annual
179 stream temperature varies between 8°C in the upstream part of the basin and 14°C in the
180 western downstream part. The majority of stations (~80%) have artificial ponds in their
181 contributing area. There are 38 stations downstream of large dams (median of distance=6
182 km). For the large dams, no information about mode-of-operation (e.g., peaking, run-of-
183 river, storage, etc.) was available. Only four stations are located downstream of natural
184 lakes (median of distance=4.15 km).

185 We obtained air temperature data from SAFRAN reanalysis at a 8-km spatial
186 resolution (Quintana-Segui et al., 2008; Vidal et al., 2010). SAFRAN is a mesoscale
187 atmospheric analysis system for surface variables. It produces an analysis at the hourly
188 time step using ground data observations and numerical models. The daily-averaged data
189 of the closest grid cell to each stream temperature station is used.

190 2.3 Basin feature databases and descriptors

191 We used four databases to obtain catchment characteristics for each station:

- 192 • BD ALTI® 50-m resolution digital terrain model dataset for topographic
193 variables (IGN, 2011);
- 194 • RHT (Theoretical Hydrographic Network for France, and its environmental
195 attributes) for river and stream hydrological variables (Pella et al., 2012);
- 196 • BD CARTHAGE® (Thematic CARTography Database of Water Agencies and
197 the Ministry of the Environment) for location and surface areas of reservoirs
198 and ponds (IGN, 2006);
- 199 • AELB (Loire-Bretagne Water Agency) for dams' characteristics (location,
200 height and volume) (Chandesris & Pella, 2006);
- 201 • SYRAH-CE (Relational System for Auditing River Hydromorphology) for
202 land cover and geomorphological variables (Valette et al., 2012).

203 3 Methods

204 We define five general steps to identify and characterize thermal signatures of
205 altered stream temperature regimes:

- 206 1. Select stream temperature stations;
- 207 2. define thermal indicators and signatures for identifying altered regimes;
- 208 3. identify thermal signatures of altered regimes through clustering based on
209 thermal indicators;
- 210 4. cross validate the derived thermal signatures; and
- 211 5. characterize the thermal signatures.

212 3.1 Select stream temperature stations

213 We selected stations based on their potential to be influenced by anthropogenic
214 structures. This effectively eliminates large rivers from our dataset because they are

215 weakly sensitive to thermal regime alterations due to their larger conveyed volumes and
216 greater thermal capacity (Smith & Lavis, 1975; Webb & Walling, 1993; Caissie, 2006;
217 Kelleher et al., 2012). Moreover, because large river temperatures are approximately in
218 equilibrium with air temperature (Moatar & Gailhard, 2006; Bustillo et al., 2014),
219 information extracted from regression-type analyses is equivocal. Therefore, this study
220 focuses on smaller rivers to identify altered regimes.

221 To subset our original dataset to focus on smaller rivers, we removed stations that are
222 in equilibrium with air temperature (and thus weakly sensitive to our proposed thermal
223 signature approach) using a distance-from-source threshold. To calculate this threshold,
224 we regressed interannual summer (June–August, referred to as “JJA” throughout)
225 temperature means for both stream and air temperature against distance from headwater
226 source (as derived from the RHT database), and extracted the intersection of the two
227 regressions (Figure S1, left panel). Sites above the distance-from-source value at this
228 intersection will be removed from further analysis.

229 *3.2 Define thermal indicators and signatures for identifying altered regimes*

230 Typically, upstream reference conditions are used to identify the downstream thermal
231 alterations of anthropogenic structures. Since such information is in practice rather
232 limited, air temperature may be used as a proxy for the heat budget reference conditions.
233 As such, we propose five thermal indicators to identify the dominant process of thermal
234 regime (Table 1 and Figure 2). The choice of these indicators is based on a preponderance
235 of literature evidence on the known impacts of dams and ponds. In the following, T_w
236 stands for stream (water) temperature and T_a for air temperature.

237 [Figure 2 about here.]

238 [Table 1 about here.]

239 The first two indicators are based on daily, summertime stream-air temperature linear

240 regressions. Stream-air temperature linear regression may be calculated on annual data
241 (Kelleher et al., 2012; Beaufort et al., 2020) or summer data (Mayer, 2012). We selected
242 the summer period to capture the higher influence of large dam operations on stream
243 temperature during these months. The first derived thermal indicator is the regression
244 slope between stream and air temperature, which we term “thermal sensitivity”, or TS ($^{\circ}\text{C}$
245 $^{\circ}\text{C}^{-1}$, or unitless [-]), because it indicates how sensitive stream temperature is to changes in
246 air temperature (Kelleher et al., 2012). In natural streams, TS is greater when climate is
247 the main control on stream temperature, but TS is lower where ground water inputs are
248 large (Caissie, 2006; Mayer, 2012) or when dams reduce the temporal coupling between
249 stream and air temperature. The second thermal indicator is the coefficient of
250 determination (R^2) of the regression between stream and air temperature, which indicates
251 the predictive capacity of air temperature on stream temperature, and therefore shows how
252 strongly these variables are coupled (Kelleher et al., 2012). In natural streams, R^2 is high,
253 whereas in streams with an upstream dam, R^2 is low, like TS.

254 The remaining three thermal indicators are derived from daily stream and air
255 temperature time series. The first one is the “lag time” (days) between the annual peak of
256 the two 30-days moving average time series. This indicator detects how dams delay the
257 annual cycle (see Figure S2 for an example). The next indicator, which we term the
258 “heating effect” ($^{\circ}\text{C}$), is the mean positive difference of daily stream-air temperature (T_w -
259 T_a) from March to October. This period is selected to avoid any snowmelt effect on stream
260 temperature, and to have the greatest increase in stream temperature due to ponds during
261 the low-flow period. This heating effect indicates how energy storage in ponds increases
262 downstream stream temperature. The final indicator, which we term the “thermal effect”
263 ($^{\circ}\text{C}$), is the mean overall difference of daily stream-air temperature difference (T_w - T_a)
264 from March to October. The thermal effect indicates overall temperature effects of ponds

265 on downstream waters, accounting for potential natural cooling and mitigation of heating
266 effects. We calculated the five indicators at each station for each year with data and
267 computed their interannual means for further analysis.

268 We hypothesized that because TS, R^2 , and lag time are able to capture the impacts of
269 managed dams—indeed, dams decrease TS and R^2 (Webb et al., 2008, and see Figure S3),
270 and delay the annual cycle (Webb & Walling, 1993; Webb, 1996)—they would reveal a
271 *dam signature* on thermal regimes (Table 1). Similarly, we hypothesized that the
272 remaining two indicators—the heating effect and the thermal effect—would detect the
273 influence of energy storage observed in the presence of artificial ponds (Dripps & Granger
274 2013, Chandesris et al. 2019, and see Figure S2), and thus reveal a *pond signature* on
275 thermal regimes (Table 1).

276 3.3 *Identify thermal signatures of altered regimes through clustering based on thermal* 277 *indicators*

278 The objective of this step is to cluster stations using the scaled values of five thermal
279 indicators defined in Table 1. We used K-means clustering (with Euclidean distance),
280 which is an unsupervised learning algorithm that partitions n observations into k clusters,
281 where each observation belongs to the cluster with the nearest mean. An optimal number
282 of clusters was obtained using the *NbClust* R package (Charrad et al., 2014; R Core Team,
283 2013). This package provides 30 popular indices that determine the number of clusters in
284 a data set by using k-means clustering method, and offers the user the best clustering
285 scheme based on different results. The number of clusters suggested by the majority of
286 these indices was selected.

287 3.4 *Cross validate derived thermal signatures*

288 We validated the derived thermal signature clusters in three ways, each based on the
289 expectation that stations clustered together would have similar catchment properties and

290 anthropogenic features. In the first step, we used a simple presence/absence test for
291 upstream human-constructions (i.e., does the station have an upstream pond or dam?). We
292 then calculated odds-ratios for each cluster from presence/absence counts of upstream
293 dams or ponds to determine the strength of association between clustering based on
294 thermal indicators and known anthropogenic influence. For example, for a cluster with a
295 dam thermal signature, we calculated the ratio between the odds of being in that cluster
296 given presence of a dam and the odds of being in the cluster given the absence of a dam.

297 Second, to test how well the clusters aligned with specific anthropogenic features, we
298 compared statistical distributions of dam and pond characteristics (Table 2) among the
299 clusters using ANOVA and the post-hoc Tukey's Honestly Significant Difference t-test
300 with Bonferroni adjustment. Prior to any analyses, we ensured homogeneity of variances
301 and normality using log transformation when necessary. Because the cross validation data
302 relies on measured dam and pond characteristics, these analyses were conducted on
303 subsets of stations with known dams (n=38) and ponds (n=260). We hypothesized that
304 stations from respective dam- or pond-like clusters would have greater or lower values of
305 their respective feature characteristics. For example, we expected that stations from the
306 dam cluster would have a much smaller distribution of distance to the closest dam than the
307 other clusters, or that stations from the pond cluster would have a higher proportion
308 ponded surface area than the other clusters. Hence, this provides a more detailed
309 validation than the simple presence/absence test.

310 Finally, we validated the dam/pond thermal signature clustering using catchment-
311 specific dam and pond characteristics in the presence of other natural landscape predictors
312 as controlling factors. To do so, we used stepwise linear regression (*MASS* package in R;
313 Venables & Ripley, 2002) to select the catchment, dam, or pond characteristics (Table 2)
314 that best explained their respective thermal indicators. We chose our catchment

315 descriptive variables based on hypothesized controls on thermal regimes, and a
316 preliminary multi-collinearity assessment using various diagnostic tests from the *mctest* R
317 package (Imdadullah et al., 2016).

318 [Table 2 about here.]

319 3.5 *Characterize the thermal signatures*

320 We first characterized the derived thermal signatures by comparing their aggregate
321 stream and air temporal behaviors. The goal was to create a portrait of how the respective
322 cumulative effects of dams and ponds modulated stream temperature relative to air
323 temperature and relative to so-called “natural” regimes. We also sought to place the
324 altered thermal regimes in the context of widely used ecological metrics. To do so, we
325 gathered metrics from biodiversity and stream ecology (Verneaux et al., 1977; Buisson &
326 Grenouillet, 2009; Steel et al., 2017; Table 3) to quantitatively evaluate anthropogenic
327 effects in altered regimes compared to natural ones. We then compared the means of these
328 thermal metrics from altered regimes to those from natural regimes using ANOVA and
329 the post-hoc Tukey’s Honestly Significant Difference t-test with Bonferroni adjustment
330 (natural regimes was used as the reference group). We excluded false-positives (e.g.,
331 stations that were clustered in a dam thermal signature, but did not have a dam) from this
332 analysis to avoid misinterpretation of true anthropogenic effects.

333 [Table 3 about here.]

334 4 **Results**

335 4.1 *Selected stations*

336 Our distance-from-source analysis found that 100 km approximately delineated the
337 designation between small and large rivers (Figure S1). Large rivers in this sense were
338 rivers with stream temperature in equilibrium with air temperature and less sensitive to the
339 human induced alterations (Figure S1, right panel). These stations are therefore excluded,

340 resulting in 330 stations with a median catchment area of 232 km² (range=3–1600 km²).

341 4.2 *Thermal indicator distributions*

342 [Figure 3 about here.]

343 Thermal indicator distributions tended to group together based on their hypothesized
344 thermal signature (i.e., dam or pond; Figure 3). TS was spatially variable across the region
345 and lacked clear patterning, although most low TS (i.e., TS<0.2) stations were located in
346 the upstream part of basin (Figure 3). In contrast, the spatial distributions of R² and lag
347 time varied much less, covaried with each other, and were more spatially homogeneous.
348 Indeed, 83% of stations had both high R² (i.e., >0.6), and short lag times (i.e., <20 days).
349 Visual inspection revealed that stations with low TS coincided with lower values of R²
350 (<0.6), and higher values of lag time (>30 days) in the upstream part of the basin. Ranges
351 for heating and thermal effects were 0.05°C to 4°C and –4.9°C to 3.7°C, respectively, but
352 the interquartile ranges were much narrower: 0.54°C to 1.14°C and -1.58 to 0.16,
353 respectively. Stations with larger heating effects (e.g., >1°C), tended to exhibit greater
354 thermal effects (e.g., >1°C) as well (r=0.9).

355 4.3 *Clustering the stations into thermal signatures*

356 The greatest proportion of indices (11 out of 30) suggested an optimal number of three
357 clusters based on the five thermal indicators. The stations in cluster 1 are located in the
358 upstream part of the basin (zone A of Figure 1). The stations in cluster 2 are scattered over
359 the basin, and 60% of the stations in cluster 3 tend to be found in the upstream part of the
360 basin (see the bottom right panel of Figure 3).

361 [Figure 4 about here.]

362 The statistical distribution of thermal indicators within each cluster suggests the proper
363 labelling of the obtained clusters with regard to the underlying physical processes (Figure
364 4). First, the lowest median values of TS (0.22) and R² (0.23) are observed in cluster 1,

365 along with the greatest median value of lag time (26 days). Therefore, we label cluster 1
366 as dam-like. Second, the greatest median values of TS (0.42), heating effect (1.38°C), and
367 thermal effect (0.65°C) are found in cluster 2. The second cluster is thus labelled as pond-
368 like. Finally, the median value of TS in stations that belong to cluster 3 (0.34) is closer to
369 the median value of TS in the stations in the pond-like cluster than that of the stations in
370 the dam-like cluster. Stations in cluster 3 also exhibit the highest median value of R^2 , and
371 the smallest heating or thermal effects. In this regard, cluster 3 is labelled as natural-like.

372 4.4 *Cross validation of derived clusters*

373 4.4.1 Presence-absence test

374 The plausibility of the clustering results was validated by the presence/absence test of
375 dams and ponds in each cluster. In support of our labelling scheme, 71% of stations in the
376 dam-like cluster had an upstream dam and if a site contained an upstream dam, it was 31.1
377 times more likely ($p < 0.001$) to be in the dam-like cluster than if it did not have an
378 upstream dam. Similarly, 94% of stations in the pond-like cluster have ponds in their
379 catchment and if a site contained an upstream pond, it was 6.5 times more likely ($p <$
380 0.001) to be in the pond-like cluster than if it did not have an upstream pond. The lower
381 odds-ratio for the pond-like cluster is due to the high proportion of stations (49% of all
382 stations) outside of this cluster that did have upstream ponds (i.e., were false negatives).
383 Indeed, 72% of stations in the natural-like cluster have ponds in their catchment.

384 4.4.2 Dam and pond characteristic distributions

385 The statistical distribution of dam descriptive variables differed from each other
386 among the clusters—IRI ($F_{1,30}=7.307$, $p=0.01$), d_{dam} ($F_{1,34}=9.120$, $p=0.005$), and $\text{IRI}/d_{\text{dam}}$
387 ($F_{1,30}=4.84$, $p=0.035$)—and clearly supported the clustering results (Figure S4). Dam-like
388 stations were located closer to their upstream dam (median=4.5 km) compared to the
389 pond-like stations (median=10 km; $t_{19}=-4.078$, $p=0.001$) and natural-like stations

390 (median=6.5 km; $t_{15}=-2.769$, $p=0.014$). Similarly, dam-like stations had upstream dams
391 that were an order of magnitude larger (implied by larger values of IRI, median=14.3%)
392 than dams upstream of pond-like stations (median=0.36%; $t_{14}=3.555$, $p=0.003$) and
393 natural-like stations (median=3.7%; $t_{17}=2.809$, $p=0.012$).

394 The mean values of pond descriptive variables also differed from each other among
395 the clusters, but the differences were less clear than for dam descriptive variables—
396 $f_{\text{pond,reach}}$ ($F_{2,205}=0.031$, $p=0.97$), $\bar{f}_{\text{pond,reach}}$ ($F_{2,205}=0.016$, $p=0.854$), and $f_{\text{pond,catchment}}$
397 ($F_{2,257}=5.967$, $p=0.003$) (Figure S5). Although statistically insignificant, pond-like
398 stations had over twice as much ponded reach area than natural like stations at both the
399 local reach scale (median $f_{\text{pond,reach}}=6.5\%$ versus 3.0% ; $t_{157}=0.235$, $p=0.815$) and the
400 catchment scale (median $\bar{f}_{\text{pond,reach}}=1.4\%$ versus 0.6% ; $t_{179}=0.557$, $p=0.578$). These results
401 were mirrored by overall proportional ponded area at the catchment scale (i.e., not just
402 along reaches) for pond-like and natural-like stations (median $f_{\text{pond,catchment}}=0.14\%$ versus
403 0.07% ; $t_{173}=3.702$, $p=0.001$). The dam-like cluster was not analyzed with t-tests because
404 we reasoned that the stream temperature regime resets at the dam position and the
405 cumulative effects of ponds will be lost.

406 4.4.3 Multiple regression with catchment variables

407 [Table 4 about here.]

408 The stepwise multiple regression procedure broadly supported the clustering
409 results, and indicated that dam and pond characteristics are the strongest controls on
410 thermal indicators and therefore on thermal signatures. Indeed, of the 10 considered
411 catchment variables, only two arose as being important predictors of or controlling
412 factors on thermal indicators (Table 4). For thermal indicators of the dam signature,
413 only lag time was influenced by catchment slope, and for the pond signature, the
414 heating effect was influenced by vegetation. More important were dam

415 characteristics: the closer a station is to a dam (low d_{dam}), and the bigger the dam
416 (high IRI) the lower the TS and R^2 ; lag time also increased at stations that were closer
417 to a dam. The influence of d_{dam} on TS was approximately 50% stronger than IRI, but
418 d_{dam} influence on R^2 was approximately 20% weaker than IRI (based on scaled regression
419 coefficients, Table 4). For lag time indicator, the influence of d_{dam} was 13% stronger than
420 catchment slope. For ponds, ponded catchment area ($f_{\text{pond,catchment}}$) was the most
421 important predictor variable of both heating and thermal effects, but percentage
422 vegetation cover (Veg%) appeared to partially mitigate heating effects (at
423 approximately half the influence of $f_{\text{pond,catchment}}$).

424 4.5 Characterize the thermal signatures

425 [Figure 5 about here.]

426 Thermal portraits from the three clusters supported current understanding on how
427 anthropogenic structures influence stream and river thermal regimes (Figure 5). Compared
428 to natural regimes, temperatures of dam-like stations exhibited downshifted (by 2°C) and
429 lagged summer thermal peaks (by 23 days), with less clear differences in winter. In
430 contrast, stream temperature of pond-like stations remains above air temperature over the
431 whole year and is nearly synchronous with air temperature, mimicking the regimes of
432 large rivers (Figure S1). Indeed, annual stream temperature amplitude of pond-like
433 stations was 14°C, 15% less than that of large rivers (16.5°C), but 30–55% greater than
434 that of dam-like or natural stations. Natural-like stations stand out in that their summer
435 peaks are cooler than pond-like stations, but are warmer and more synchronous with air
436 temperature than dam-like stations.

437 [Figure 6 about here.]

438 Altered thermal regimes (i.e., dam- and pond-like) clearly separated from natural
439 regimes along ecological metrics— $\bar{T}_{w,\text{summer}}$ ($F_{322}=17.625$, $p<0.001$), $\max(T_{w,\text{month}})$

440 ($F_{322}=20.719$, $p<0.001$), $N_{T_w>20}$ ($F_{322}=55.529$, $p<0.001$), $D_{T_w>15}$ ($F_{320}=38.928$, $p<0.001$),
441 and $\max(\Delta T_w)$ ($F_{322}=39.786$, $p<0.001$). Magnitude and frequency ($\bar{T}_{w,\text{summer}}$ and $N_{T_w>20}$)
442 thermal metrics were less for dam-like stations than for natural-like stations (by 2°C ,
443 $t_{15}=3.633$, $p=0.02$; and 4 days, $t_{32}=4.204$, $p=0.001$), but frequency, duration, and rate of
444 change thresholds were equivocal (Figure 6).

445 Altered thermal regimes from ponds differed from natural regimes along every thermal
446 metric considered here, with a 2.3°C increase in average $\bar{T}_{w,\text{summer}}$ ($t_{182}=-11.603$,
447 $p<0.001$), a 2.5°C increase in $\max(T_{w,\text{month}})$ ($t_{169}=-9.3$, $p<0.001$), a 15-day increase in
448 $N_{T_w>20}$ ($t_{104}=-9.504$, $p<0.001$), a 39-day increase in $D_{T_w>15}$ ($t_{150}=-10.119$, $p<0.001$), and a
449 2.6°C increase in ΔT_w ($t_{210}=-12.345$, $p<0.001$).

450 5 Discussion

451 Our results demonstrate that five simple indicators derived from stream-air
452 temperature time series are capable of identifying the extent and characteristics of both
453 altered and natural stream thermal regimes. Using these indicators, we could accurately
454 parse the divergent thermal signatures of dams and ponds on the thermal regimes of
455 flowing waters.

456 5.1 Large dam thermal signature

457 The spatial clustering of dam thermal signatures into the upstream of the Loire River
458 basin aligned with the known distribution of dams there (Figure 1). This thermal signature
459 approach may therefore be useful in identifying areas with strong thermal alteration from
460 dam proliferation, like in the Amazon headwaters (Anderson et al. 2018).

461 Dam mode of operation affects its degree of change in downstream thermal regime
462 (Olden & Naiman, 2010; Maheu et al., 2016a) and should be reflected in its emergent
463 thermal signature. Our observed dam thermal signature was based on hypothesized
464 cooling effects from hypolimnetic release, and although most stations downstream of

465 large dams exhibited this signature, many did not, suggesting alternative modes of
466 operation. Hence, in future works, subsequent use of alternative thermal indicators to
467 capture other modes of operation may be warranted. Even dams with the same purpose
468 could have different mode of operation (Maheu et al., 2016a). Interannual variability
469 driven by climate, adding an additional layer of complexity that may be difficult to assess
470 with this method. Regardless, even the relatively simple approach here was largely
471 successful in identifying altered thermal regimes. We provide additional evidence here
472 that dams which release hypolimnetic water disrupt the stream-air temperature
473 relationship (R^2) (Buendía et al. 2015), and delay the annual stream temperature peak
474 (Olden & Naiman, 2010) (Figures 4 and 5).

475 The degree of dam thermal alterations depends on reservoir volume, stream order, and
476 distance from the dam (Webb et al., 2008; Batalla et al., 2004). Here, we also show that
477 channel slope is an important compounding factor on dam influence, which appeared to
478 amplify lag time effects from dam proximity (Table 4): the steeper the channel, the less
479 travel time there is for water-air equilibrium and thermal lag time increases. Our cross
480 validation results also highlight the critical effect of dam volume on thermal regimes,
481 underscoring previous works that identified a critical impoundment threshold of 5–20% of
482 the mean annual runoff (Buendía et al. 2015; Maheu et al. 2016a). Importantly, we found
483 that $IRI > 20\%$ completely erased stream-air temperature correlation (data not shown; cf.
484 Buendía et al. 2015). Stations with the weakest dam signature were far from large dams,
485 supporting the known reduction of dams influence on thermal regimes (increase of TS)
486 with distance due to the heat exchange with ambient conditions (Preece & Jones, 2002;
487 Buendía et al., 2015). The coupling of greater distance from dam and lower IRI of
488 upstream dam may provide additional explanation as to why 17 stations with known dams
489 did not cluster into our dam-like thermal signature.

490 The induced changes by dams in ecologically relevant thermal metrics on downstream
491 temperature were moderate. We observed effects of decreased summer stream
492 temperatures and a large decrease in the frequency of high temperatures, in accordance
493 with previous works (Olden & Naiman, 2010; Maheu et al., 2016a), but found little
494 evidence for other ecologically relevant effects compared to natural systems. However,
495 our focus was biased towards increased thermal alterations, and further metrics and
496 analysis would benefit future inference.

497 *5.2 Pond thermal signature*

498 Ponds and shallow (<15 m in height) reservoirs impound water for different purposes
499 that depend on location and local needs. We observed that ponds were evenly distributed
500 throughout the Loire basin, with no clear clustering of sizes (Figure 1, right panel). In
501 support of this observation, pond-like thermal signatures were evident throughout the
502 basin (Figure 3), located mostly on medium size streams (median of distance from
503 source=40 km).

504 Ponds typically release warm water from overflow, increasing downstream
505 temperatures synchrony with air temperature (Dripps & Granger 2013, Maheu et al.,
506 2016b). The pond thermal signature identified here aligns with other empirical results
507 (Chandesris et al., 2019) and this general conceptual model (Figures 4 and 5). Stations
508 influenced by small dams experience a small decrease in R^2 , compared to natural stations
509 (cf. Bae et al., 2016), which we also observed to a small degree (Figure 4). The extent of
510 the induced change by ponds depends mostly on the surface area and residence time
511 (Maxted et al., 2005; Chandesris et al., 2019). The lack of data on the depth of the
512 pond/shallow reservoirs at this scale prevented us from using residence time. A bigger
513 surface area, or a bigger residence time increase the time of exposure to air temperature
514 and incoming solar radiation, leading to greater sensitivity of stream temperature to air

515 temperature (increased TS) (Maheu et al., 2016b; Michel et al., 2020). We also detected
516 greater TS (thermal sensitivity) for pond-like stations (see Figure 4).

517 The single best predictor of the pond thermal signature was the proportion of a
518 station's catchment that was ponded, strongly implying that pond effects have an
519 emergent, cumulative effect on stream temperature regimes. Indeed, of the local, reach-
520 scale metrics, neither could differentiate the thermal indicators or signatures (Table 4,
521 Figure S5). However, we note that the reach scale metrics were defined based on recorded
522 surface waters in 2011 and are perhaps not temporally aligned with stream and air
523 temperature measurements used here. Importantly, our cross validation suggests that the
524 thermal influence of ponds may be mitigated by vegetation cover (Maxted et al., 2005),
525 suggesting the strategic planting of canopy cover species in thermal restoration efforts.

526 Ponds can alter ecologically relevant thermal metrics substantially. They increase the
527 summer temperatures, frequency and duration of high temperatures (Lessard & Hayes,
528 2003; Maheu et al., 2016a, 2016b; Chandesris et al. 2019) which we found as well (see
529 Figure 6).

530 5.3 *Natural regimes*

531 The thermal regimes of natural-like stations are those that are most strongly driven by
532 natural factors like climate, topography, vegetative shading, and stream discharge (Poole
533 & Berman, 2001; Kelleher et al., 2012; Hannah & Garner, 2015). These thermal
534 signatures should therefore arise in regions with minimal anthropogenic influence, which
535 we observed in their spatial clustering predominately in the upstream part of the Loire
536 River basin where there is the greatest proportion of vegetation cover (cf. Beaufort et al.,
537 2020). These natural stations were located on smaller streams (median of distance from
538 source=24 km) and had typically greater proportions of vegetative cover (median of
539 vegetation cover within a 10 meter buffer=100%).

540 Natural-like thermal signatures, unlike altered ones, had strong correlation with air
541 temperature (cf. Webb et al., 2008) and exhibited minimal lag time, heating, or thermal
542 effects (Figure 4). In accordance with Beaufort et al. (2020), who studied the controlling
543 factors of natural regimes the Loire River basin, TS at the stations located on large rivers
544 where climate is the key driver of stream temperature (median=0.43), was greater than the
545 TS in natural-like stations (median=0.34). However, the values of TS in our study were
546 smaller than the TS values reported by Beaufort et al. (2020), since the present study has
547 focused on summer TS values. A similar result (median of TS=0.45) was obtained in an
548 analysis focused on August stream temperatures, that attributed decreased summer TS to
549 ground water input (Mayer 2012). In the current study, TS in the stations located in region
550 B (Figure 1), which has the greatest potential for ground water input, was lower than TS
551 in the stations located in regions A, and C (median TS=0.29 versus 0.35). Supporting our
552 thermal signature approach, we observed annual amplitude for stations with natural
553 thermal signatures (median=11°C) in direct accordance of observations in Beaufort et al.,
554 (2020) (9–14°C).

555 *5.4 Limitations of the study*

556 The stream temperature database used in the current study only includes stations with
557 complete annual data, but less complete databases may struggle with the outlined
558 approach. For example, when we also included 170 stations that only had summer data in
559 our analysis, we observed that the lag time indicator was highly sensitive to within-year
560 data availability, indicating that a year-round dataset is required for clustering. However,
561 the pond signature indicators (heating and thermal effects) were not sensitive to within-
562 year data availability, even when the summer stream temperature data were available.
563 Importantly, if complete annual data are not available, the indicators appear quite robust
564 to interannual data heterogeneity (i.e., missing whole years of data; Figure S6). The only

565 exception is lag time indicator, which can be heavily influenced by year-to-year variations
566 in both climate and upstream reservoir management.

567 The large sample size used in the present study, the presence of different types of
568 reservoirs over the study area, and the blind-eye towards dam operation may have some
569 implications for generalizing our findings. For example, in regions with more variable
570 dam operations, different clusters may arise, or it may be difficult to perform cluster
571 analysis without additional thermal indicators. Scales of inference are also likely to vary
572 among regions. In our study, we had a low possibility of station pseudo-replication due to
573 high resolution of SAFRAN data (8 km): only 20% of the SAFRAN meshes included
574 more than one station, and only 12% of the meshes included the stations with the same
575 clustering group. Hence, it is imperative to verify and cross-validate this approach when
576 applied to new datasets.

577 *5.5 Implications and perspectives*

578 The proposed thermal signatures approach allows a simple, rapid, and accurate
579 workflow to identify river reaches that are highly influenced by dams and ponds. The
580 methodology is inherently regional, aligning in scale with the jurisdictions of most
581 environmental agencies and working groups. We suggest that thermal signature results
582 can be used to identify hotspots and target specific reaches for restoration and further
583 investigation, and to more broadly design strategic measurement networks (Jackson et al.,
584 2016). Thermal signatures can also identify natural reaches as benchmarks for restoration
585 or aquatic species habitat protection. Indeed, there is much interest in predicting the
586 phenological and spatial diversity within species of interest or their prey (Steel et al.,
587 2017). Moreover, because climate change will likely exacerbate the degree of thermal
588 alterations (Michel et al., 2020) through increasing air temperature, decreasing
589 streamflow, and increasing demand for ponds and dams (Webb, 1996; Moatar & Gailhard,

590 2006), the thermal signature framework could be used to plan pond and dam placement to
591 minimize cumulative downstream effects.

592 The proposed thermal signatures may also be used by modelers to develop a reference-
593 condition model by the use of natural regimes (Hill et al., 2013), or to assess the
594 performance of distributed water temperature models that do not take into account
595 anthropogenic activities. The differences between simulated and observed thermal
596 signatures at altered stations can serve as a bias correction factor that is a function of
597 known dam or pond descriptive variables.

598 The thermal signature approach is flexible and can easily be reimaged for the other
599 purposes other than detection and characterization of altered regimes from anthropogenic
600 impoundments. For example, the stream-air temperature linear regression calculated on
601 annual data could identify varied thermal signatures of ground water inputs in natural
602 streams (with a focus on TS and the intercept) (Kelleher et al., 2012; Beaufort et al.,
603 2020). Moreover, the synthesis of thermal signatures and hydrological signatures could be
604 applicable in analyzing fish and macroinvertebrate communities.

605 **6 Conclusions**

606 Thermal signatures enable rapid and clear evaluation of the cumulative impact of
607 human impoundments on stream temperature, highlighting two dominant modes of
608 thermal alteration in the Loire River basin. We expect that the application of the thermal
609 signatures will reveal new, possibly overlooked, modes of alteration depending on where
610 it is applied, resulting in new perspectives on the growing spatiotemporal effects of
611 anthropogenic structures to thermal regimes. Ultimately, by identifying natural thermal
612 regimes, thermal signatures provide important information to managers on reference
613 conditions, and can be used in conjunction with distributed models to identify bias,
614 leading to improved performance and predictive capacity.

615 **7 Acknowledgements**

616 This work was realized in the course of a doctoral project at University of Tours,
617 funded by European Regional Development Fund (Fonds Européen de développement
618 Régional-FEDER) POI FEDER Loire no2017- EX001784, and Le plan Loire grandeur
619 nature, Agence de l'eau Loire-Bretagne (AELB). The SAFRAN database was provided by
620 the French national meteorological service (Météo-France). Stream temperature data were
621 provided by the Office français de la biodiversité (OFB) and Fédération de Pêche (fishing
622 federation).

623 **8 References**

- 624 Anderson, E. P., Jenkins, C. N., Heilpern, S., Maldonado-Ocampo, J. A., Carvajal-
625 Vallejos, F. M., Encalada, A. C., ... & Salcedo, N. (2018). Fragmentation of Andes-
626 to-Amazon connectivity by hydropower dams. *Science Advances*, 4(1), eaao1642.
- 627 Bae, M. J., Merciai, R., Benejam, L., Sabater, S., & García-Berthou, E. (2016). Small
628 weirs, big effects: disruption of water temperature regimes with hydrological
629 alteration in a Mediterranean stream. *River Research and Applications*, 32(3), 309-
630 319. doi: <https://doi.org/10.1002/rra.2871>.
- 631 Batalla, R. J., Gomez, C. M., & Kondolf, G. M. (2004). Reservoir-induced hydrological
632 changes in the Ebro River basin (NE Spain). *Journal of Hydrology*, 290(1-2), 117-
633 136. doi: <https://doi.org/10.1016/j.jhydrol.2003.12.002>.
- 634 Beaufort, A., Moatar, F., Sauquet, E., Loicq, P., & Hannah, D. M. (2020). Influence of
635 landscape and hydrological factors on stream–air temperature relationships at
636 regional scale. *Hydrological Processes*, 34(3), 583-597. doi:
637 <https://doi.org/10.1002/hyp.13608>.
- 638 Berhanu, B., Seleshi, Y., Demisse, S. S., & Melesse, A. M. (2015). Flow regime
639 classification and hydrological characterization: a case study of Ethiopian rivers.
640 *Water*, 7(6), 3149-3165. doi: <https://doi.org/10.3390/w7063149>.
- 641 Boon, P. J., & Shires, S. W. (1976). Temperature studies on a river system in north-east

642 England. *Freshwater Biology*, 6(1), 23-32. doi: <https://doi.org/10.1111/j.1365->
643 [2427.1976.tb01587.x](https://doi.org/10.1111/j.1365-2427.1976.tb01587.x).

644 Buendía, C., Sabater, S., Palau, A., Batalla, R. J., & Marcé, R. (2015). Using equilibrium
645 temperature to assess thermal disturbances in rivers. *Hydrological Processes*,
646 29(19), 4350-4360. doi: [https://onlinelibrary.wiley.com/
647 doi/epdf/10.1002/hyp.10489](https://onlinelibrary.wiley.com/doi/epdf/10.1002/hyp.10489).

648 Buisson, L., & Grenouillet, G. (2009). Contrasted impacts of climate change on stream
649 fish assemblages along an environmental gradient. *Diversity and Distributions*,
650 15(4), 613-626. doi: <https://doi.org/10.1111/j.1472-4642.2009.00565.x>.

651 Bustillo, V., Moatar, F., Ducharne, A., Thiéry, D., & Poirel, A. (2014). A multimodel
652 comparison for assessing water temperatures under changing climate conditions via
653 the equilibrium temperature concept: case study of the Middle Loire River, France.
654 *Hydrological Processes*, 28(3), 1507-1524..doi: <https://doi.org/10.1002/hyp.9683>.

655 Caissie, D., St-Hilaire, A., & El-Jabi, N. (2004, June). Prediction of water temperatures
656 using regression and stochastic models. In *57th Canadian Water Resources
657 Association Annual Congress., Montreal (Vol. 6)*.

658 Caissie, D. (2006). The thermal regime of rivers: a review. *Freshwater biology*, 51(8),
659 1389-1406. doi: <https://doi.org/10.1111/j.1472-4642.2009.00565.x>.

660 Casado, A., Hannah, D. M., Peiry, J. L., & Campo, A. M. (2013). Influence of dam-
661 induced hydrological regulation on summer water temperature: Sauce Grande
662 River, Argentina. *Ecohydrology*, 6(4), 523-535. doi: [https://doi.org/
663 10.1002/eco.1375](https://doi.org/10.1002/eco.1375).

664 Chandesris, A., & Pella, H. (2006). Constitution d'une base d'information spatialisée
665 «barrages, retenues et plans d'eau» au niveau national en vue d'évaluer les
666 modifications hydro-morphologiques (Doctoral dissertation, irstea). URL:
667 <https://hal.inrae.fr/hal-02587668>.

668 Chandesris, A., Van Looy, K., Diamond, J. S., & Souchon, Y. (2019). Small dams alter
669 thermal regimes of downstream water. *Hydrology and Earth System Sciences*, 23,

670 4509-4525. doi: <https://doi.org/10.5194/hess-23-4509-2019>.

671 Charrad, M., Ghazzali, N., Boiteau, V., Niknafs, A., & Charrad, M. M. (2014).
672 Package 'nbclust'. *Journal of statistical software*, 61, 1-36. doi:
673 <http://dx.doi.org/10.18637/jss.v061.i06>

674 Cheng, Y., Voisin, N., Yearsley, J. R., & Nijssen, B. (2020). Reservoirs modify river
675 thermal regime sensitivity to climate change: a case study in the southeastern
676 United States. *Water Resources Research*, 56(6), e2019WR025784. doi:
677 <https://doi.org/10.1029/2019WR025784>.

678 Cox, T. J., & Rutherford, J. C. (2000). Predicting the effects of time-varying
679 temperatures on stream invertebrate mortality. *New Zealand Journal of Marine
680 and Freshwater Research*, 34(2), 209-215. doi: [https://doi.org/10.
681 1080/00288330.2000.9516927](https://doi.org/10.1080/00288330.2000.9516927).

682 Daniels, M. E., & Danner, E. M. (2020). The Drivers of River Temperatures Below a
683 Large Dam. *Water Resources Research*, 56(5), e2019WR026751. doi:
684 <https://doi.org/10.1029/2019WR026751>.

685 Dripps, W., & Granger, S. R. (2013). The impact of artificially impounded, residential
686 headwater lakes on downstream water temperature. *Environmental Earth Sciences*,
687 68(8), 2399-2407. doi: [https://doi.org/10.1007/
688 s12665-012-1924-4](https://doi.org/10.1007/s12665-012-1924-4).

688 Ducharne, A. (2008). Importance of stream temperature to climate change impact on
689 water quality. URL: <https://hal.archives-ouvertes.fr/hal-00330876>.

690 Dugdale, S. J., Hannah, D. M., & Malcolm, I. A. (2017). River temperature modelling: A
691 review of process-based approaches and future directions. *Earth-Science Reviews*,
692 175, 97-113. doi: <https://doi.org/10.1016/j.earscirev.2017.10.009>.

693 Erickson, T. R., & Stefan, H. G. (2000). Linear air/water temperature correlations for
694 streams during open water periods. *Journal of Hydrologic Engineering*, 5(3),
695 317-321. doi: [https://doi.org/10.1061/\(ASCE\)1084-0699\(2000\)5:3\(317\)](https://doi.org/10.1061/(ASCE)1084-0699(2000)5:3(317)).

696 Fraley, J. J. (1979). Effects of elevated stream temperatures below a shallow reservoir on
697 a cold water macroinvertebrate fauna. In *The ecology of regulated streams* (pp.

698 257-272). Springer, Boston, MA. doi: [https://doi.org/10.1007/978-1-4684-8613-](https://doi.org/10.1007/978-1-4684-8613-1_15)
699 1_15.

700 Grantz, E. M., Haggard, B. E., & Scott, J. T. (2014). Stoichiometric imbalance in
701 rates of nitrogen and phosphorus retention, storage, and recycling can
702 perpetuate nitrogen deficiency in highly-productive reservoirs. *Limnology and*
703 *Oceanography*, 59(6), 2203-2216. doi:
704 <https://doi.org/10.4319/lo.2014.59.6.2203>.

705 Gupta, H. V., Wagener, T., & Liu, Y. (2008). Reconciling theory with observations:
706 elements of a diagnostic approach to model evaluation. *Hydrological Processes: An*
707 *International Journal*, 22(18), 3802-3813. doi: <https://doi.org/10.1002/hyp.6989>.

708 Habets, F., Boé, J., Déqué, M., Ducharne, A., Gascoin, S., Hachour, A., Martin, E.,
709 Pagé, C., Sauquet, E., Terray, L. and Thiéry, D. (2013). Impact of climate change
710 on the hydrogeology of two basins in northern france. *Climatic change*, 121 , 771–
711 785. doi: <https://doi.org/10.1007/s10584-013-0934-x>.

712 Hannah, D. M., & Garner, G. (2015). River water temperature in the United
713 Kingdom: changes over the 20th century and possible changes over the 21st
714 century. *Progress in Physical Geography*, 39(1), 68-92. doi: <https://doi.org/10.1177/2F0309133314550669>.

715

716 Harrison, J. A., Maranger, R. J., Alexander, R. B., Giblin, A. E., Jacinthe, P. A.,
717 Mayorga, E., ... & Wollheim, W. M. (2009). The regional and global
718 significance of nitrogen removal in lakes and reservoirs. *Biogeochemistry*,
719 93(1-2), 143-157. doi: <https://doi.org/10.1007/s10533-008-9272-x>.

720 Hill, R. A., Hawkins, C. P., & Carlisle, D. M. (2013). Predicting thermal reference
721 conditions for USA streams and rivers. *Freshwater Science*, 32(1), 39-55. doi:
722 <https://doi.org/10.1899/12-009.1>.

723 IGN (2006). Descriptif technique bd carthage. URL:
724 https://geoservices.ign.fr/ressources_documentaires/Espace_documentaire/BAS
725 [ES_VECTORIELLES/BDCARTHAGE/DL_BDCARTHAGE_3_0.pdf](https://geoservices.ign.fr/ressources_documentaires/Espace_documentaire/BAS_ES_VECTORIELLES/BDCARTHAGE/DL_BDCARTHAGE_3_0.pdf)

726 IGN (2011). Descriptif technique bd alti, URL:
727 https://geoservices.ign.fr/ressources_documentaires/Espace_documentaire/MO
728 [DELES_3D/BDALTIV2/DC_BDALTI_2-0.pdf](https://geoservices.ign.fr/ressources_documentaires/Espace_documentaire/MO)

729 Imdadullah, M., Aslam, M., & Altaf, S. (2016). mctest: An R Package for Detection of
730 Collinearity among Regressors. *R J.*, 8(2), 495.

731 Jackson, F. L., Malcolm, I. A., & Hannah, D. M. (2016). A novel approach for
732 designing large-scale river temperature monitoring networks. *Hydrology*
733 *Research*, 47(3), 569-590. doi: <https://doi.org/10.2166/nh.2015.106>.

734 Kelleher, C., Wagener, T., Gooseff, M., McGlynn, B., McGuire, K., & Marshall, L.
735 (2012). Investigating controls on the thermal sensitivity of Pennsylvania
736 streams. *Hydrological Processes*, 26(5), 771-785. doi: [https://doi.org/](https://doi.org/10.1002/hyp.8186)
737 [10.1002/hyp.8186](https://doi.org/10.1002/hyp.8186).

738 Lamouroux, N., Pella, H., Vanderbecq, A., Sauquet, E., & Lejot, J. (2010). Estimkart 2.0:
739 Une plate-forme de modèles écohydrologiques pour contribuer à la gestion des
740 cours d'eau à l'échelle des bassins français. Version provisoire. Cemagref, Agence
741 de l'Eau Rhône-Méditerranée-Corse, Onema, Lyon (45 pp.).

742 Le Moal, Morgane, Chantal Gascuel-Odoux, Alain Ménesguen, Yves Souchon,
743 Claire Étrillard, Alix Levain, Florentina Moatar et al. (2019). Eutrophication: a
744 new wine in an old bottle?. *Science of the Total Environment*, 651, 1-11. doi:
745 <https://doi.org/10.1016/j.scitotenv.2018.09.139>.

746 Lehner, B., Liermann, C. R., Revenga, C., Vörösmarty, C., Fekete, B., Crouzet, P., ... &
747 Nilsson, C. (2011). High-resolution mapping of the world's reservoirs and dams for
748 sustainable river-flow management. *Frontiers in Ecology and the Environment*,
749 9(9), 494-502. doi: [10.1890/100125](https://doi.org/10.1890/100125).

750 Lessard, J. L., & Hayes, D. B. (2003). Effects of elevated water temperature on fish and
751 macroinvertebrate communities below small dams. *River research and applications*,
752 19(7), 721-732. doi:<https://doi.org/10.1002/rra.713>.

753 Lowney, C. L. (2000). Stream temperature variation in regulated rivers: Evidence for

754 a spatial pattern in daily minimum and maximum magnitudes. *Water Resources*
755 *Research*, 36(10), 2947-2955. doi: <https://doi.org/10.1029/2000WR900142>.

756 Maheu, A., St-Hilaire, A., Caissie, D., El-Jabi, N., Bourque, G., & Boisclair, D. (2016a).
757 A regional analysis of the impact of dams on water temperature in medium-size
758 rivers in eastern Canada. *Canadian Journal of Fisheries and Aquatic Sciences*, 73 ,
759 1885–1897. doi: <https://doi.org/10.1139/cjfas-2015-0486>.

760 Maheu, A., St-Hilaire, A., Caissie, D., & El-Jabi, N. (2016b). Understanding the thermal
761 regime of rivers influenced by small and medium size dams in Eastern Canada.
762 *River Research and Applications*, 32(10), 2032-2044. doi:
763 <https://doi.org/10.1002/rra.3046>.

764 Maxted, J. R., McCready, C. H., & Scarsbrook, M. R. (2005). Effects of small ponds
765 on stream water quality and macroinvertebrate communities. *New Zealand*
766 *Journal of Marine and Freshwater Research*, 39(5), 1069-1084. doi:
767 <https://doi.org/10.1080/00288330.2005.9517376>.

768 Mayer, T. D. (2012). Controls of summer stream temperature in the Pacific Northwest.
769 *Journal of Hydrology*, 475, 323-335. doi:
770 <https://doi.org/10.1016/j.jhydrol.2012.10.012>.

771 McMillan, H., Westerberg, I., & Branger, F. (2017). Five guidelines for selecting
772 hydrological signatures. doi: <https://doi.org/10.1002/hyp.11300>.

773 Michel, A., Brauchli, T., Lehning, M., Schaefli, B., & Huwald, H. (2020). Stream
774 temperature and discharge evolution in Switzerland over the last 50 years:
775 annual and seasonal behaviour. *Hydrology and earth system sciences*, 24(1),
776 115-142. doi: <https://doi.org/10.5194/hess-24-115-2020>.

777 Minaudo, C., Curie, F., Jullian, Y., Gassama, N., & Moatar, F. (2018). QUAL-NET, a
778 high temporal-resolution eutrophication model for large hydrographic networks.
779 *Biogeosciences*, 15(7). doi: <https://doi.org/10.5194/bg-15-2251-2018>.

780 Moatar, F., & Gailhard, J. (2006). Water temperature behaviour in the River Loire since
781 1976 and 1881. *Comptes Rendus Geoscience*, 338(5), 319-328. doi:

782 <https://doi.org/10.1016/j.crte.2006.02.011>.

783 Mohseni, O., Erickson, T. R., & Stefan, H. G. (1999). Sensitivity of stream temperatures
784 in the United States to air temperatures projected under a global warming scenario.
785 *Water Resources Research*, 35(12), 3723-3733. doi: 10.1029/1999WR900193.

786 Niemeyer, R. J., Cheng, Y., Mao, Y., Yearsley, J. R., & Nijssen, B. (2018). A thermally
787 stratified reservoir module for large-scale distributed stream temperature models
788 with application in the Tennessee River Basin. *Water Resources Research*, 54(10),
789 8103-8119. doi: <https://doi.org/10.1029/2018WR022615>.

790 O'Driscoll, M. A., & DeWalle, D. R. (2006). Stream–air temperature relations to classify
791 stream–ground water interactions in a karst setting, central Pennsylvania, USA.
792 *Journal of Hydrology*, 329(1-2), 140-153. doi: <https://doi.org/10.1016/j.jhydrol.2006.02.010>.

793

794 Olden, J. D., & Naiman, R. J. (2010). Incorporating thermal regimes into environmental
795 flows assessments: modifying dam operations to restore freshwater ecosystem
796 integrity. *Freshwater Biology*, 55(1), 86-107. doi: <https://doi.org/10.1111/j.1365-2427.2009.02179.x>.

797

798 Pella, H., Lejot, J., Lamouroux, N., & Snelder, T. (2012). Le réseau hydrographique
799 théorique (RHT) français et ses attributs environnementaux. *Géomorphologie: relief, processus, environnement*, 18(3), 317-336. doi:
800 <https://doi.org/10.4000/geomorphologie.9933>.

801

802 Petts, G. E., & Gurnell, A. M. (2005). Dams and geomorphology: research progress
803 and future directions. *Geomorphology*, 71(1-2), 27-47. doi:
804 <https://doi.org/10.1016/j.geomorph.2004.02.015>.

805 Pilgrim, J. M., Fang, X., & Stefan, H. G. (1998). STREAM TEMPERATURE
806 CORRELATIONS WITH AIR TEMPERATURES IN MINNESOTA:
807 IMPLICATIONS FOR CLIMATE WARMING 1. *JAWRA Journal of the American Water Resources Association*, 34(5), 1109-1121 doi:
808 <https://doi.org/10.1111/j.1752-1688.1998.tb04158.x..>

809

810 Poole, G. C., & Berman, C. H. (2001). Profile: an ecological perspective on in-stream
811 temperature: natural heat dynamics and mechanisms of human-cause thermal
812 degradation. *Journal of Environmental Management*, 27, 787-802. doi: <https://doi.org/10.1007/s002670010188>.
813

814 Preece, R. M., & Jones, H. A. (2002). The effect of Keepit Dam on the temperature
815 regime of the Namoi River, Australia. *River Research and Applications*, 18(4), 397-
816 414. doi: <https://doi.org/10.1002/rra.686>.

817 Quintana-Segui, P., Le Moigne, P., Durand, Y., Martin, E., Habets, F., Baillon, M., ...
818 & Morel, S. (2008). Analysis of near-surface atmospheric variables: Validation
819 of the SAFRAN analysis over France. *Journal of applied meteorology and*
820 *climatology*, 47(1), 92-107. doi: <https://doi.org/10.1175/2007JAMC1636.1>.

821 Team, R. C. (2013). R: A language and environment for statistical computing. URL:
822 <http://www.R-project.org/>.

823 Sauquet, E., & Catalogne, C. (2011). Comparison of catchment grouping methods for
824 flow duration curve estimation at ungauged sites in France. doi: 10.5194/hess-15-
825 2421-2011.

826 Sauquet, E., Gottschalk, L., & Leblois, E. (2000). Mapping average annual runoff: a
827 hierarchical approach applying a stochastic interpolation scheme. *Hydrological*
828 *sciences journal*, 45(6), 799-815. doi: <https://doi.org/10.1080/02626660009492385>.

829 Schmadel, N. M., Harvey, J. W., Alexander, R. B., Schwarz, G. E., Moore, R. B., Eng,
830 K., ... & Scott, D. (2018). Thresholds of lake and reservoir connectivity in river
831 networks control nitrogen removal. *Nature communications*, 9(1), 1-10. doi:
832 <https://doi.org/10.1038/s41467-018-05156-x>.

833 Sinokrot, B. A., Stefan, H. G., McCormick, J. H., & Eaton, J. G. (1995). Modeling of
834 climate change effects on stream temperatures and fish habitats below dams and
835 near groundwater inputs. *Climatic Change*, 30(2), 181-200. doi:
836 <https://doi.org/10.1007/BF01091841>.

837 Smith, K., & Lavis, M. E. (1975). Environmental influences on the temperature of a

838 small upland stream. *Oikos*, 228-236. doi: <https://doi.org/10.2307/3543713>.

839 Steel, E. A., Beechie, T. J., Torgersen, C. E., & Fullerton, A. H. (2017). Envisioning,
840 quantifying, and managing thermal regimes on river networks. *BioScience*, 67(6),
841 506-522. doi: <https://doi.org/10.1093/biosci/bix047>.

842 Steel, E. A., & Lange, I. A. (2007). Using wavelet analysis to detect changes in water
843 temperature regimes at multiple scales: Effects of multi-purpose dams in the
844 Willamette River basin. *River Research and Applications*, 23(4), 351-359. doi:
845 <https://doi.org/10.1002/rra.985>.

846 Stefan, H. G., & Preud'homme, E. B. (1993). Stream temperature estimation from air
847 temperature 1. *JAWRA Journal of the American Water Resources Association*,
848 29(1), 27-45. doi: <https://doi.org/10.1111/j.1752-1688.1993.tb01502.x>.

849 Valette, L., Piffady, J., Chandesris, A., & Souchon, Y. (2012). SYRAH-CE: description
850 des données et modélisation du risque d'altération hydromorphologique des cours
851 d'eau pour l'état des lieux DCE. Rapport Technique Onema-Irstea. URL:
852 http://oai.afbiodiversite.fr/cindocoai/download/PUBLI/1185/1/2012_108.pdf_4080
853 Ko.

854 Van Vliet, M. T. H., Yearsley, J. R., Franssen, W. H. P., Ludwig, F., Haddeland, I.,
855 Lettenmaier, D. P., & Kabat, P. (2012). Coupled daily streamflow and water
856 temperature modelling in large river basins. *Hydrology and Earth System Sciences*,
857 16(11), 4303-4321. doi: 10.5194/hess-16-4303-2012.

858 Venables, W. N., & Ripley, B. D. (2002). *Modern Applied Statistics with S* 4th ed New
859 York Springer. URL: <http://www.stats.ox.ac.uk/pub/MASS4>.

860 Verneaux, J. (1977). BIOTYPOLOGIE DE L'ECOSYSTEME" EAU COURANTE".
861 DETERMINISME APPROCHE DE LA STRUCTURE BIOTYPOLOGIQUE.

862 Vidal, J. P., Martin, E., Franchistéguy, L., Baillon, M., & Soubeyroux, J. M. (2010). A
863 50-year high-resolution atmospheric reanalysis over France with the Safran system.
864 *International Journal of Climatology*, 30(11), 1627-1644. doi:
865 <https://doi.org/10.1002/joc.2003>.

866 Vörösmarty, C. J., Meybeck, M., Fekete, B., Sharma, K., Green, P., & Syvitski, J. P.
867 (2003). Anthropogenic sediment retention: major global impact from registered
868 river impoundments. *Global and planetary change*, 39(1-2), 169-190. doi:
869 [https://doi.org/10.1016/S0921-8181\(03\)00023-7](https://doi.org/10.1016/S0921-8181(03)00023-7).

870 Yearsley, J. R., Sun, N., Baptiste, M., & Nijssen, B. (2019). Assessing the impacts of
871 hydrologic and land use alterations on water temperature in the Farmington River
872 basin in Connecticut. *Hydrology and Earth System Sciences*, 23(11), 4491-4508.
873 doi: <https://doi.org/10.5194/hess-23-4491-2019>.

874 Webb, B. W. (1996). Trends in stream and river temperature. *Hydrological processes*,
875 10(2), 205-226. doi: [https://doi.org/10.1002/\(SICI\)1099-1085\(199602\)10:2<205::AID-HYP358>3.0.CO;2-1](https://doi.org/10.1002/(SICI)1099-1085(199602)10:2<205::AID-HYP358>3.0.CO;2-1).

876 Webb, B. W., & Walling, D. E. (1993). Temporal variability in the impact of river
877 regulation on thermal regime and some biological implications. *Freshwater*
878 *Biology*, 29(1), 167-182. doi: <https://doi.org/10.1111/j.1365-2427.1993.tb00752.x>.

880 Webb, B. W., & Walling, D. E. (1996). Long-term variability in the thermal impact of
881 river impoundment and regulation. *Applied Geography*, 16(3), 211-223. doi:
882 [https://doi.org/10.1016/0143-6228\(96\)00007-0](https://doi.org/10.1016/0143-6228(96)00007-0).

883 Webb, B. W., & Walling, D. E. (1997). Complex summer water temperature behaviour
884 below a UK regulating reservoir. *Regulated Rivers: Research & Management: An*
885 *International Journal Devoted to River Research and Management*, 13(5), 463-477.
886 doi: [https://doi.org/10.1002/\(SICI\)1099-1646\(199709/10\)13:5<463::AID-RRR470>3.0.CO;2-1](https://doi.org/10.1002/(SICI)1099-1646(199709/10)13:5<463::AID-RRR470>3.0.CO;2-1).

887 Webb, B. W., & Zhang, Y. (1997). Spatial and seasonal variability in the components of
888 the river heat budget. *Hydrological processes*, 11(1), 79-101. doi:
889 [https://doi.org/10.1002/\(SICI\)1099-1085\(199701\)11:1<79::AID-HYP404>3.0.CO;2-N](https://doi.org/10.1002/(SICI)1099-1085(199701)11:1<79::AID-HYP404>3.0.CO;2-N).

890 Webb, B. W., Hannah, D. M., Moore, R. D., Brown, L. E., & Nobilis, F. (2008). Recent
891 advances in stream and river temperature research. *Hydrological Processes: An*

List of Figures

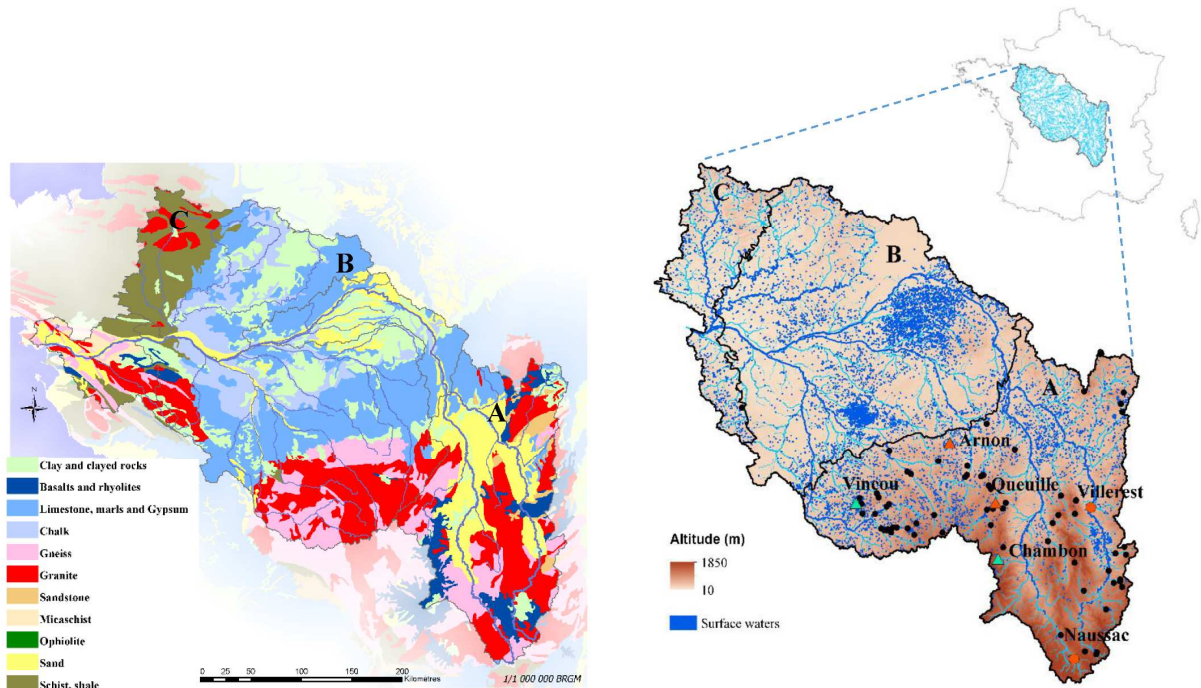


Figure 1: The Loire River basin. Left panel: main aquifer formations and basin lithology; granite and basalt dominate the upstream part of the basin (Region A), whereas sedimentary rocks occupy the middle reaches with a potential for ground water input (Region B), which leads to more granite and schist in the lower reaches (Region C). Right panel: altitude and surface waters. Black points show dams higher than 15 m. Red circle points show the two largest dams in the basin. Triangles denote stations that had a potential for upstream-downstream comparison (red for dams, green for ponds), which are visually assessed in Supplementary Figure 2.

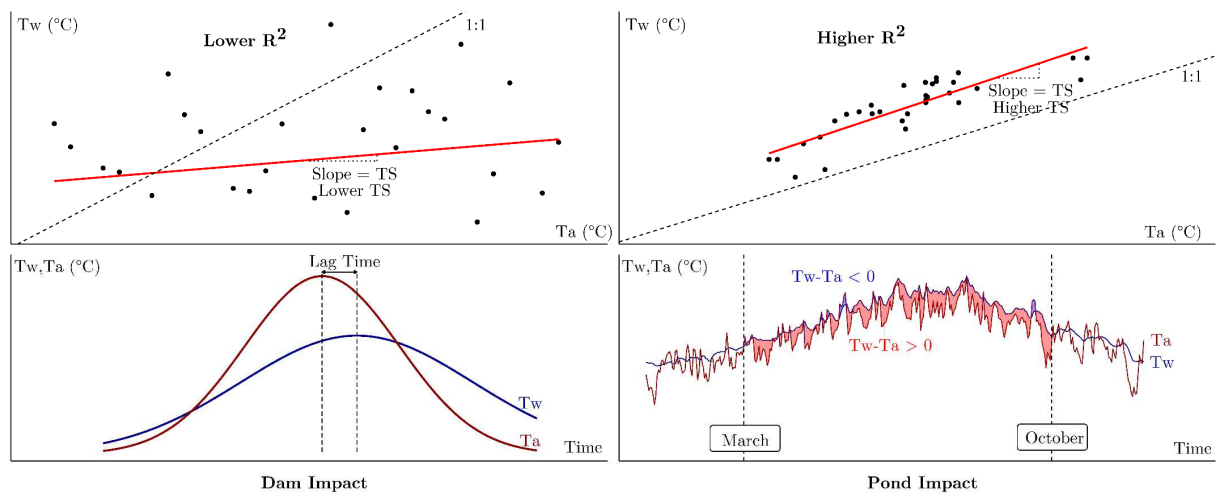


Figure 2: Conceptual representation of thermal signatures. Top row: daily stream-air temperature linear regression showing lower TS (Thermal Sensitivity) and lower R^2 downstream of a dam (left), and higher TS and higher R^2 downstream of ponds (right). Bottom row: stream and air temperature regimes showing the lagged annual cycle of stream temperature relative to air temperature downstream of a dam (left), and greater heating effect and thermal effect more often downstream of ponds (right). See Table 1 for the mathematical definition of thermal signatures.

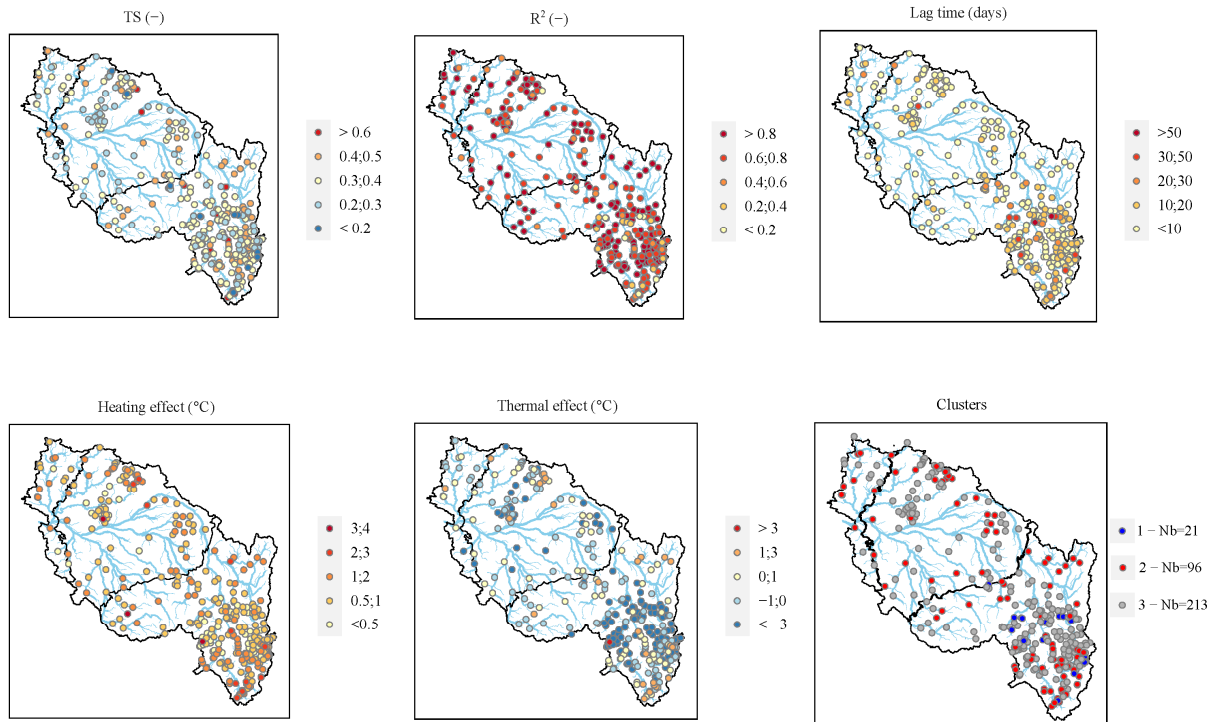


Figure 3: Spatial distribution of the five thermal indicator values over 330 stations on the Loire basin, and spatial distribution of the stations in three obtained clusters, or thermal signatures (bottom right). The top row were expected dam thermal indicators and the bottom row (i.e., heating and thermal effects) were expected pond thermal indicators.

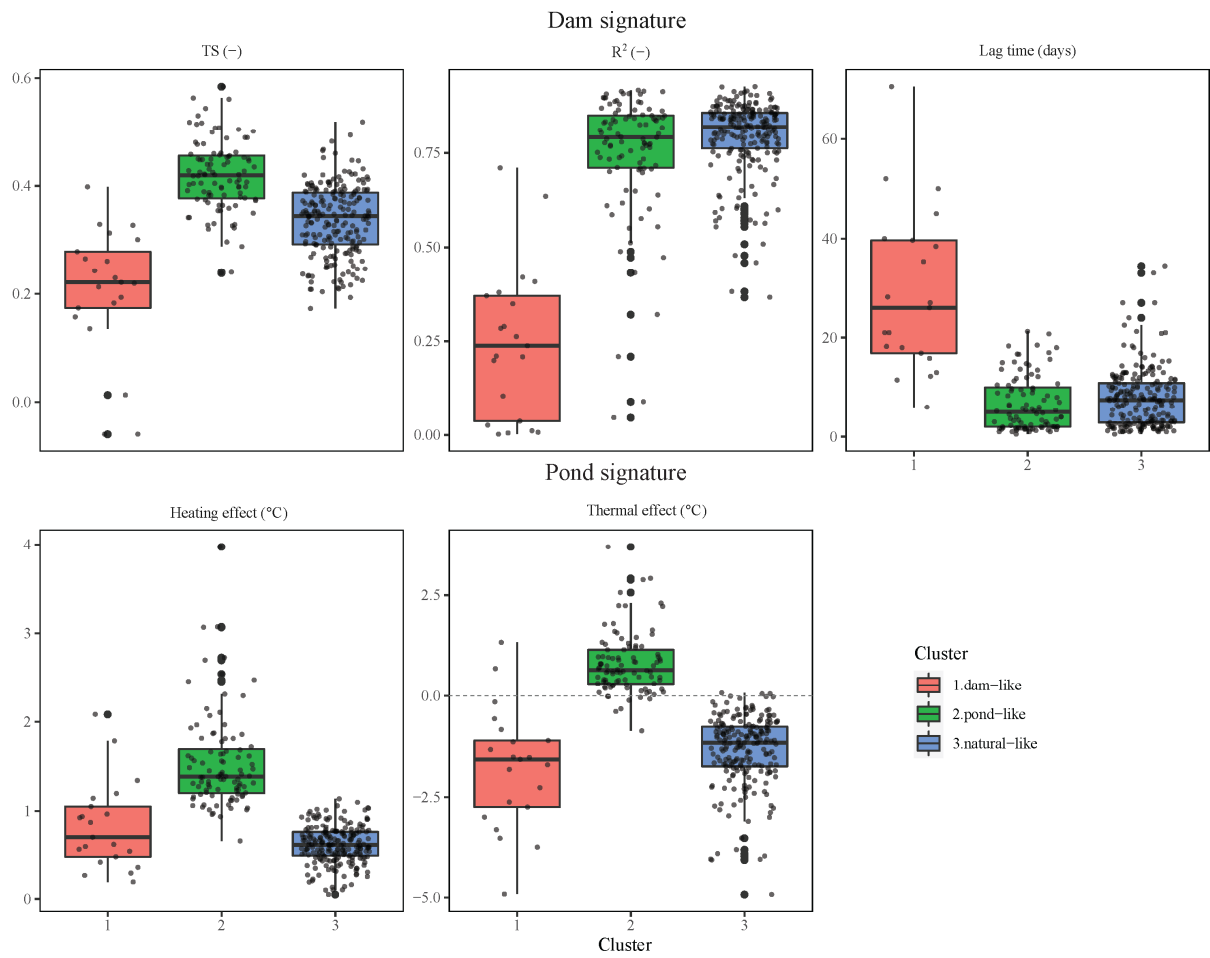


Figure 4: Statistical distribution of thermal signatures in each cluster: 1.dam-like with 21 stations; 2.pond-like with 96 stations; 3.natural-like with 213 stations.

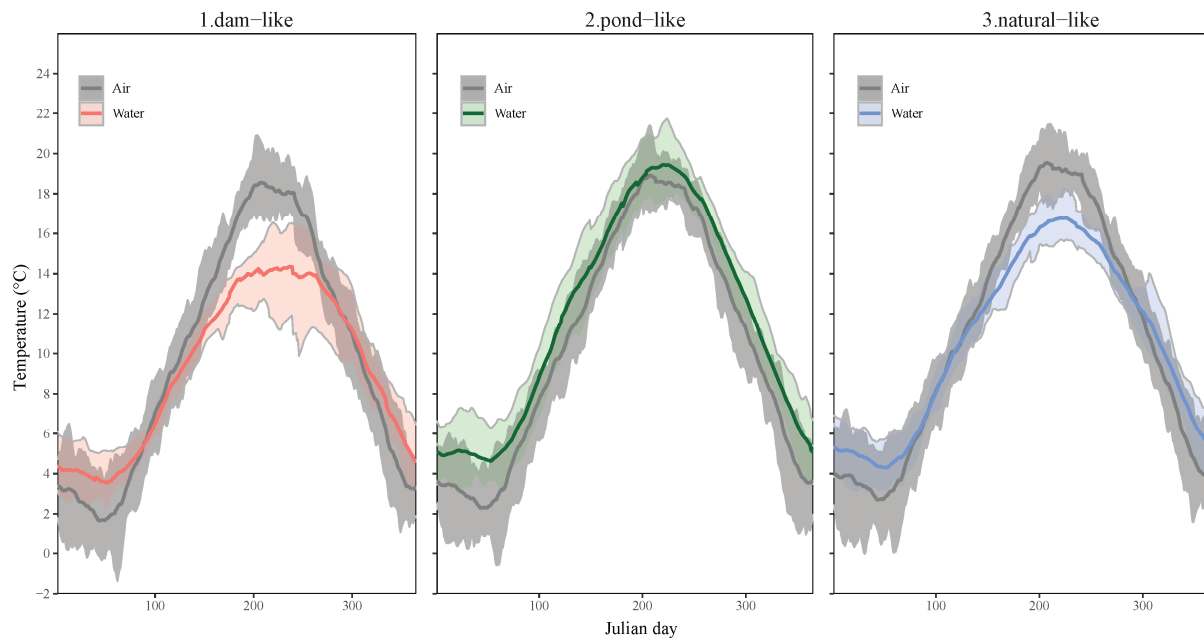


Figure 5: The annual air and water temperature regimes of altered (by dams and ponds) and natural streams. Shaded areas represent the 10th-90th percentile band, and solid lines represent the median value: 1.dam-like with 15 stations that have a large upstream dam; 2.pond-like with 90 stations; 3.natural-like with 213 stations.

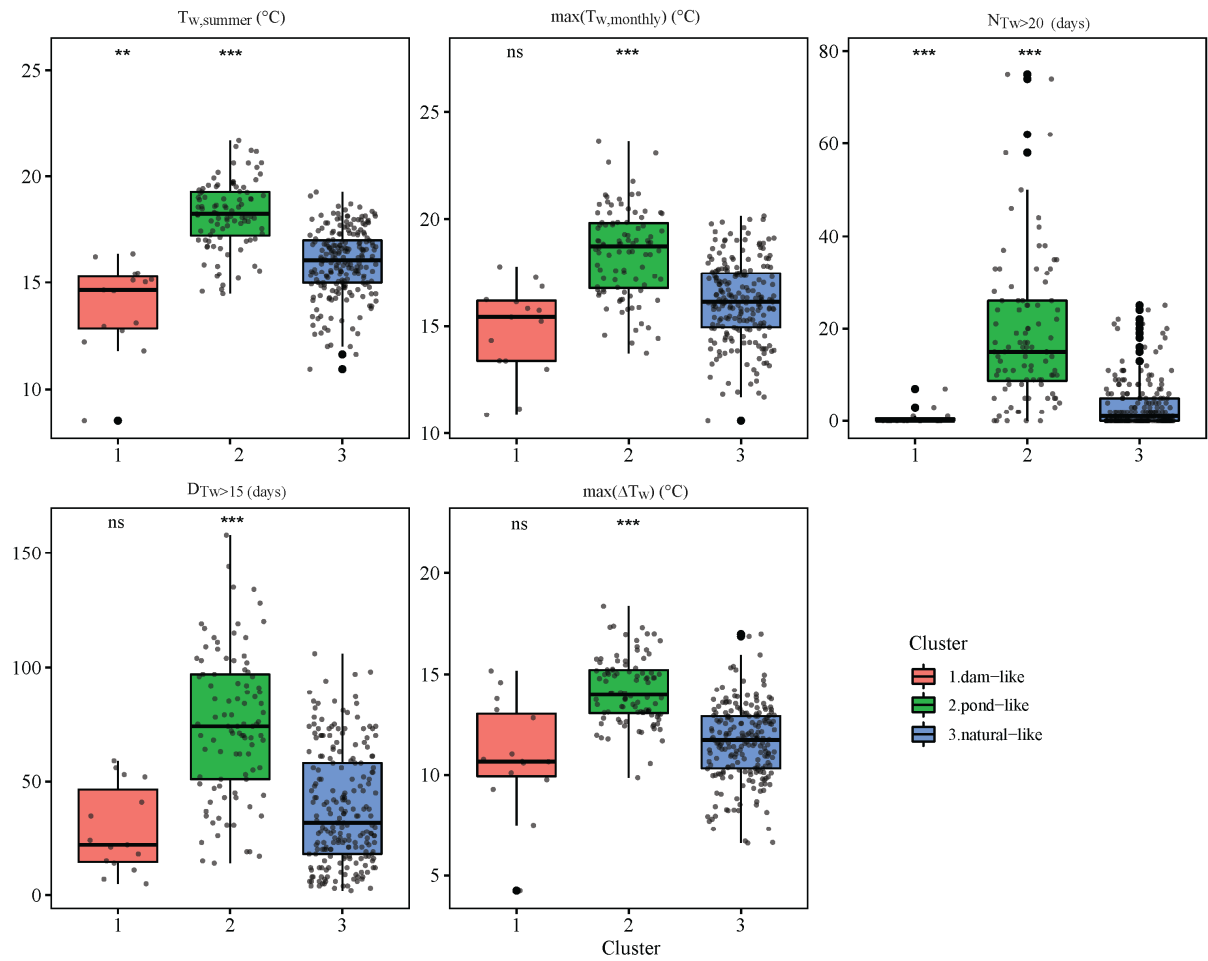


Figure 6: Statistical distribution of ecologically relevant thermal metrics in each cluster: 1) dam-like with 15 stations that have a large upstream dam, 2) pond-like with 90 stations, and 3) natural-like with 213 stations. The t-test was conducted with the reference group of natural-like cluster. ***, **, and * indicates that the metric for the group of altered regimes is significantly different from natural regimes at the 1, 5 and 10% confidence levels, respectively. The “ns” shows that the metric for the group of altered regime is non-significantly different from natural regimes.

List of Tables

Table 1: Indicators used to identify thermal signatures of altered stream temperature regimes. Indicators are grouped into a dam or pond signature based on their hypothesized ability to detect thermal effects from their respective anthropogenic structures.

Indicator	Definition	Rationale
Dam signature		
Thermal sensitivity (TS)	Daily JJA stream-air temperature linear regression slope	Dams reduce TS
R ²	Daily JJA stream-air temperature coefficient of determination	Dams reduce R ²
Lag time	Lag time between the annual peak in 30-days moving average stream and air temperature regimes	Dams increase lag time
Pond signature		
Heating effect	mean positive difference of daily stream-air temperature difference ($T_w - T_a$) from March–October	Ponds increase distributed energy storage, leading to heating
Thermal effect	mean overall difference of daily stream-air temperature difference ($T_w - T_a$) from March–October	Ponds increase energy storage, even in the presence of natural cooling

Note: Indicators are calculated based on interannual averages

Table 2: Descriptive variables tested for assessing the links between thermal signatures and dam/pond characteristics (see Section 3.4). Mean and standard deviation values (SD) are shown for the 330 stations selected in the study (see Section 3.1).

Notation	Variable	Mean	SD	Unit
dam/pond characteristics				
d_{dam}	Distance from the closest large dam ^a	6.6	4.2	km
IRI	Impounded Runoff Index of the closest large dam ^b	11	16	%
$\text{IRI}/d_{\text{dam}}$	IRI/distance from the closest large dam ^c	10	25.5	%/km
$f_{\text{pond,reach}}$	Fraction of station's reach surface area that is ponded ^d	7.5	12	%
$\bar{f}_{\text{pond,reach}}$	Fraction of station's reach surface area that is ponded; averaged over all upstream reaches	1.6	2.7	%
$f_{\text{pond,catchment}}$	Fraction of the catchment area that is ponded ^e	0.17	0.8	%
catchment properties				
T_a	Annual mean T_a at station	12	1.5	°C
$A_{\text{catchment}}$	Catchment area	232	300	km ²
Alt	Altitude at station	399	290	m
S	Upstream mean slope	0.037	0.03	m/km
D	Distance from the source	30	20	km
W_q	Width for median discharge ^f	8.7	6.3	m
D_q	Depth for median discharge ^f	0.3	0.16	m
q	Mean annual specific discharge ^g	10	4.9	l/s/km ²
CI	Connectivity index ^h	0.4	0.08	-
Veg	Rate of vegetation cover ⁱ	83	22	%

^a Derived from ArcMap tools.

^b Ratio of dam volume to mean annual runoff.

^c To capture the interaction between the dam characteristic and the position of a station from the dam.

^d Extracted from SYRAH-CE database (Valette et al., 2012). Final nodes of each considered river segment are at important confluences and topologically important places.

^e A proxy of cumulative effects of upstream ponds.

^f From the ESTIMKART empirical model developed by Lamouroux et al. (2010).

^g Based on geostatistical interpolation on the RHT network (Pella et al., 2012; Sauquet et al., 2000).

^h IC: Q10-Q99/Q1-Q99; represents the shape of the dimensionless flow duration curve. This descriptor is a measure of the contrast between low-flow and high-flow regimes. Values close to 1 are observed where there are large aquifers or storage in snow packs. Values close to 0 are related to catchments exposed to contrasted weather (Sauquet & Catalogne, 2011).

ⁱ Derived from remote sensing on both sides of reaches with a buffer of 10 m at station, as reported in SYRAH-CE database (Valette et al., 2012).

Table 3: Selected ecologically relevant thermal metrics for comparison between altered regimes and natural ones.

Regime feature	Metric	Description	Biological importance
Magnitude	$\bar{T}_{w, \text{summer}}$	Mean T_w in summer (June–August)	Differences in mean temperature across river systems contribute to determining which species are present and which are absent
	$\max(T_{w, \text{monthly}})$	Maximum of the 30-day moving average daily mean T_w	Used in the biotypology according to the formula proposed by Verneaux et al. (1977)
Frequency	$N_{T_w > 20}$	Number of days that daily mean $T_w > 20^\circ\text{C}$	Species-specific differences in response to high temperatures provide preferential advantages to particular species
Duration	$D_{T_w > 15}$	Duration of consecutive days with mean $T_w > 15^\circ\text{C}$	Accumulated stress may trigger migration and other major life-history transitions
Rate of change	$\max(\Delta T_w)$	Difference between mean T_w in August and February	The competitive advantage of one species over another may be determined by conditions in both summer and winter ^a

^a Buisson & Grenouillet (2009) used air temperature instead of water temperature.

Table 4: Stepwise multiple linear regression results for cross-validation approach relating descriptive variables for thermal indicators within dam and pond signatures. ***, **, and * denote significance at the 1, 5 and 10% confidence levels, respectively. The scaled coefficients are shown in parentheses for comparison among predictor variables.

Dam signature			
Descriptive variable	TS (-)	R² (-)	Lag time (days)
S [m/km]	—	—	232.85±92.891** (0.377±0.151)
d _{dam} [km]	0.015±0.005*** (0.458±0.140)	0.029±0.010** (0.385±0.141)	-1.6±0.560*** (-0.425±0.151)
IRI [%]	-0.002±0.001** (-0.306±0.145)	-0.009±0.002*** (-0.484±0.146)	—
Adjusted R ²	0.43	0.482	0.3
F statistic (df)	12.37 (29)	15.43 (29)	7.64 (29)
p-value	<0.001	<0.001	0.002
Pond signature			
Descriptive variable	Heating effect (°C)	Thermal effect (°C)	
Veg [%]	-0.003±0.002* (-0.164±0.102)	—	
f _{pond,catchment} [%]	0.62±0.211*** (0.296±0.102)	0.762±0.305** (0.257±0.102)	
Adjusted model R ²	0.1	0.060	
F statistic (df)	5.442 (87)	3.872 (87)	
p-value	0.006	0.024	

